Authors
Oliver Meseguer-Ruiz
Departamento de Ciencias Históricas y Geográficas, Universidad de Tarapacá
Climatology Group, University of Barcelona
ORCID: 0000-0002-2222-6137
Email: omeseguer@academicos.uta.cl

Paulina I. Ponce-Philimon
Departamento de Ciencias Históricas y Geográficas, Universidad de Tarapacá
Email: paulina.pphilimon@gmail.com

Alan S. Quispe-Jofré
Departamento de Ciencias Históricas y Geográficas, Universidad de Tarapacá
Email: alanjofreq@gmail.com

Jose A. Guijarro
State Meteorological Agency (AEMet), Balearic Islands Office, Spain
ORCID: 0000-0002-9527-9758
Email: jguijarrop@aemet.es

Pablo Sarricolea
Departamento de Geografía, Universidad de Chile
Climatology Group, University of Barcelona
ORCID: 0000-0002-6679-2798
Email: psarricolea@uchilefau.cl

Title

Spatial behaviour of daily observed extreme temperatures in Northern Chile (1966-2015): data quality, warming trends, and its orographic and latitudinal effects

Corresponding author
Oliver Meseguer-Ruiz
2222, 18 de septiembre, Arica, Chile
E-mail: omeseguer@academicos.uta.cl
Telephone: +56 5 8220 5255

Abstract

According to the Intergovernmental Panel on Climate Change (IPCC), Northern Chile will be one of the most affected territories by changes in the atmospheric dynamics in next years. These climate change effects will be noticed in several ways, and temperatures will be one of the most sensitive variables to these changes, and with high importance because of their relationship with the hydrological cycle in one of the most arid regions in the world. Extreme temperatures of 77 observatories have been analysed by the calculation of 14 indices and their temporal trends. Also, the relationship of these indices between them, between observatories, with elevation and latitude has been taken into consideration, while they imply significant differences of the behaviour of the analysed indices. The results showed general warming trends but with particular differences depending on the behaviour of minimum temperatures. Examining the relationship between the indices and elevation, it appears that this variable has more implications in minimum temperatures. The analysis showed significant correlations also between the indices and latitude, agreeing with not evident general warming trends in the intertropical area of Northern Chile. Considering the different behaviours of the trends and their relationships with latitude and elevations, it has to be analysed in the future the possible existing relations with the spatial and temporal changes in the hydrological cycle such as precipitations.

Keywords
Altiplano, Atacama Desert, climate change, spatial correlation, temporal changes.

1. Introduction

Temperatures show a spatial distribution dependent on multiple factors. This is evidenced according to the temporal variability shown in observed data in regions with homogeneous climates (Maraun et al. 2017). Daily and annual variability in temperatures respond to natural cycles, day / night and summer / winter respectively, but extremes in temperatures may have severe effects on human activities and health, and have been previously observed (Trenberth et al. 2007; IPCC 2013).

Effects of extreme temperatures can influence several environmental aspects, like crop growth, agro ecological regionalization and food supply (Ye et al. 2013, Tian et al. 2017). Extreme temperatures over critical thresholds may also cause a rise in the incidence of mortality (Keellings and Waylen 2012). The hydrological cycle is also affected by natural cycles, more intense precipitation can modify a river's regime, ground humidity and evapotranspiration balances (Labat et al. 2004, Zhai et al. 2005, Guan et al. 2015, Donat et al. 2016). According to observations, global warming across the 20^{th} Century, has been demonstrated by a large number of studies in different regions worldwide, at different scales, globally (Vose et al. 2005) and local (Caloiero 2016).

The behaviour of extreme temperatures have been widely studied in the last recent years in several regions in the world (Abatan et al. 2017; Caloiero et al. 2017; Gabaldón-Leal et al. 2017; Salman et al. 2017, Rahimi and Hejabi 2017). Benefits of studying extreme temperatures instead of mean temperatures have been demonstrated (Villarini et al. 2017). In South America, these studies are fewer, and concern mostly the south of the continent (Berman et al. 2013; Jacques-Coper and Brönniman 2014). In Peru, a recent study has been published using a monthly gridded data set of maximum and minimum temperatures in order to identify significant trends over the last 50 years (Vicente-Serrano et al. 2017). The results showed that maximum air temperatures increased in summer but decreased in winter, with a clear elevation-warming dependency, with the strongest warming recorded at highly elevated sites, but for minimum temperatures trends, this dependency is weakened, showing lower magnitudes of warming trends or even cooling trends. Arid regions are consequently more sensitive to global warming (Donat et al. 2016) as its affects may have more severe implications to natural processes and economic systems. If global warming modifies the hydrological cycle in Northern Chile (17°S - 29°S) (Held and Soden 2006), it could further affect the on-going drought conditions (Sarricolea and Romero 2015, Sarricolea et al. 2017). This area faces a rising water demand scenario associated with the economic development of the country, as well as the increase of population in urban areas, and more especially to mining activities in the Atacama Desert. This activity provides Chile high economic benefits. Important mining projects have been developed in the area in recent years, intensifying water demands and creating high competitiveness with other economic activities such as the traditional ranching in high areas or agriculture located in coastal valleys (Sarricolea and Romero 2015). It is generally accepted that this detected observed warming has an anthropogenic origin (Barkhordarian et al. 2017).

But the last few years have shown a slowdown in warming trends which is not totally explained (Karl et al. 2015): some authors say that the sensitivity of the climate system has been overestimated (Otto et al. 2013), others (Cowtan and Way 2014) affirm that it is explained by the lack of observations in areas where there is not a good density of meteorological stations, or even explained by changes in solar activity and in tropospheric and stratospheric aerosols in the last decade (Solomon et al. 2011, Santer et al. 2014). However, evidence suggests that the energy surplus has been kept in the oceans (Meehl et al. 2011, Guemas et al. 2013), particularly in the Equatorial Pacific (Kosaka and Xie 2013) related to the Pacific Decadal Oscillation (PDO) cold phase and the strengthening of the trade winds (Trenberth and Fasullo 2013, England et al. 2014, Meehl et al. 2014).

Despite this, there is no other region in the world where this warming slowdown is so evident that in the coast of northern Chile (Vuille et al. 2015) and its high elevated areas (Bennett et al. 2016), where temperature has experienced a fall of 0.20 ºC /decade in the last 20-30 years (Falvey and Garreaud 2009, Schulz et al. 2012) after a significant rise during the first part of the 20^{th} Century (Rosenblüth et al. 1997). This cooling was partially explained by changes in the PDO and the further intensification of the South Pacific High (SPH) and the cold water upwelling streams beneath the thermocline, which would normally cool down the region (Falvey and Garreaud 2009). Despite this, Andean glaciers keep retreating (Rabatel et al. 2013, Durán-Alarcón et al. 2015), so new reanalysis of the data have been undertaken in some of the Andes regions (Schauwecker et al. 2014).

Meanwhile, temperature across the tropical Pacific west coast (Perú and Ecuador) rose to maximum values in the second half of the 20^{th} Century (Marengo et al. 2011). Other studies at a regional scale showed significant warming trends at the same time in the Andes of Peru (Lavado Casimiro et al. 2013, Salzmann et al. 2013, Schauwecker et al. 2017), Bolivia (Seiler et al. 2013) and Colombia (Poveda and Pineda 2009). Despite this, it has been demonstrated that this slowdown in the general warming trends between 2002 and 2014 is contemporary with an acceleration of ice melting, suggesting a redistribution of heat within the atmosphere-ocean-cryosphere system (Berger et al. 2017). Consequently, it seems that some differences exist between observed temperatures trends in the inter-tropical areas and the mid-latitudes ones, and between the continents warming far from the coasts and the cooling of the oceans. It is still uncertain if the recent anomalous cooling affects only the mid-latitudes of the Pacific coast of South America or its effects extend to tropical regions too. More ancient studies (Vuille and Bradley 2000) do not detect this cooling, due because the 20th Century data were used, not including the cooling period. Simulated results according to CMIP model show significant changes into warming at the end of the 21st Century for neighbour areas in Bolivia (Thibeault et al. 2010).

Observations of climate variables in high areas are not very frequent (Beniston et al. 1997), but Northern Chile has a significant number of meteorological stations in areas located over 2,000 m.a.s.l. (Figure 1). In South America, some studies have analysed the behaviour of precipitations at high altitudes, as mentioned above. But similar projects have been developed in similar areas in the world, linked to the analysis of the behaviour of mountain glaciers and snow cover. Those studies have mainly focused on the Tibetan Plateau (Liang et al. 2014, Cai et al. 2016, Shen et al. 2017, Kattel and Yao 2018), Middle-East (Parak et al. 2015, Rahimi and Hejabi 2017) and Central Asia (Feng et al. 2017, Shrestha et al. 2017). All these studies agree and indicate general warming trends. These high mountain systems cover about one-fifth of the Earth's continental areas and are all inhabited to a greater or lesser extent except for Antarctica (Beniston et al. 1997). These systems also provide direct support for close of the 10% of the world's population. The exhibit within short horizontal distances, climatic regimes which are similar to those of widely separated latitudinal belts; they consequently are very interesting to study areas, in the way they represent such different responses to climate change effects. Hence the importance of having a good quality database of observed data.

A similar study has been carried out in Central Chile (Burger et al. 2018), to the south of the area of interest of the present work. In this case, only two observations were considered above 2,000 m.a.s.l. Significant positive trends in mean annual temperature between 1979 and 2015 are identified at valley sites, but trends are non-significant at all other stations. Significant positive trends in annual maximum temperature are found at most of the observatories except in high areas in the Andes and the coastal stations, with a significant maximum temperature cooling trend recorded on the coast around 30°S. In contrast, annual minimum temperature exhibits significant warming only in metropolitan areas, while valley stations at a range of latitudes show significant cooling trends, with non-significant trends in minimum temperature recorded at remaining stations. There is a general pattern of maximum temperatures rising faster than minimum temperatures at valley sites outside metropolitan areas, significantly increasing daily temperature amplitude. In contrast, on the coast, the decreasing trend of maximum temperature has resulted in a decrease in daily temperature range.

The aim of this study was to obtain a good quality database of observed data in the study area. After that, we analyse the trends of maximum and minimum daily temperatures and to consider the magnitude and the spatial distribution of the extremes in Northern Chile for the period 1966-2015 and according to 14 indices proposed by the Expert Team on Climate Change Detections Indices (ETCCDI) (Zhang et al. 2011). We also aim to review the relationship of these trends between them, of each meteorological station with each other, and also with altitude and latitude in the region. This will allow us to see if the effects of these two geographic components show any general warming trends or are modified or not by other factors. It also aims to identify if the changing temperatures of the region are sensitive to the complex orography where it is not yet well-determined so it can inform policymakers and hydrologists in their decisions concerning water supplies in an area where water represents a very scarce resource.

This work presents in the first place the techniques used to obtain good quality datasets, and after that the analysis of the spatial behaviour of well-known indices based on extreme temperatures, which provides more accurate information about this atmospheric variable, traditionally analysed through mean values. Identify regional variations of these observed temperatures is of high interest, especially in a region with a very complex orography and very elevated areas. This study presents a description of the used data and the methods carried out through the study, another section with the obtained results and their comparison with other studies, and a final section with the main conclusions.

2. Data and methods

Data and analysis were based on 77 meteorological observatories pertaining to the Chilean Meteorological Direction (DMC) and the Water General Direction (DGA) both in Northern Chile, located as shown in Figure 1.

Data were gathered for the period 1950-2015, but their availability along this period is very varied among the stations, ranging from 1 to 99 %. Fig. 2 shows the data coverage individually (2a) and globally (2b). Temperatures also exhibit a great variation in the 77 series, with mean values (calculated on the raw series) ranging from 1.1 to 20.1 Celsius.

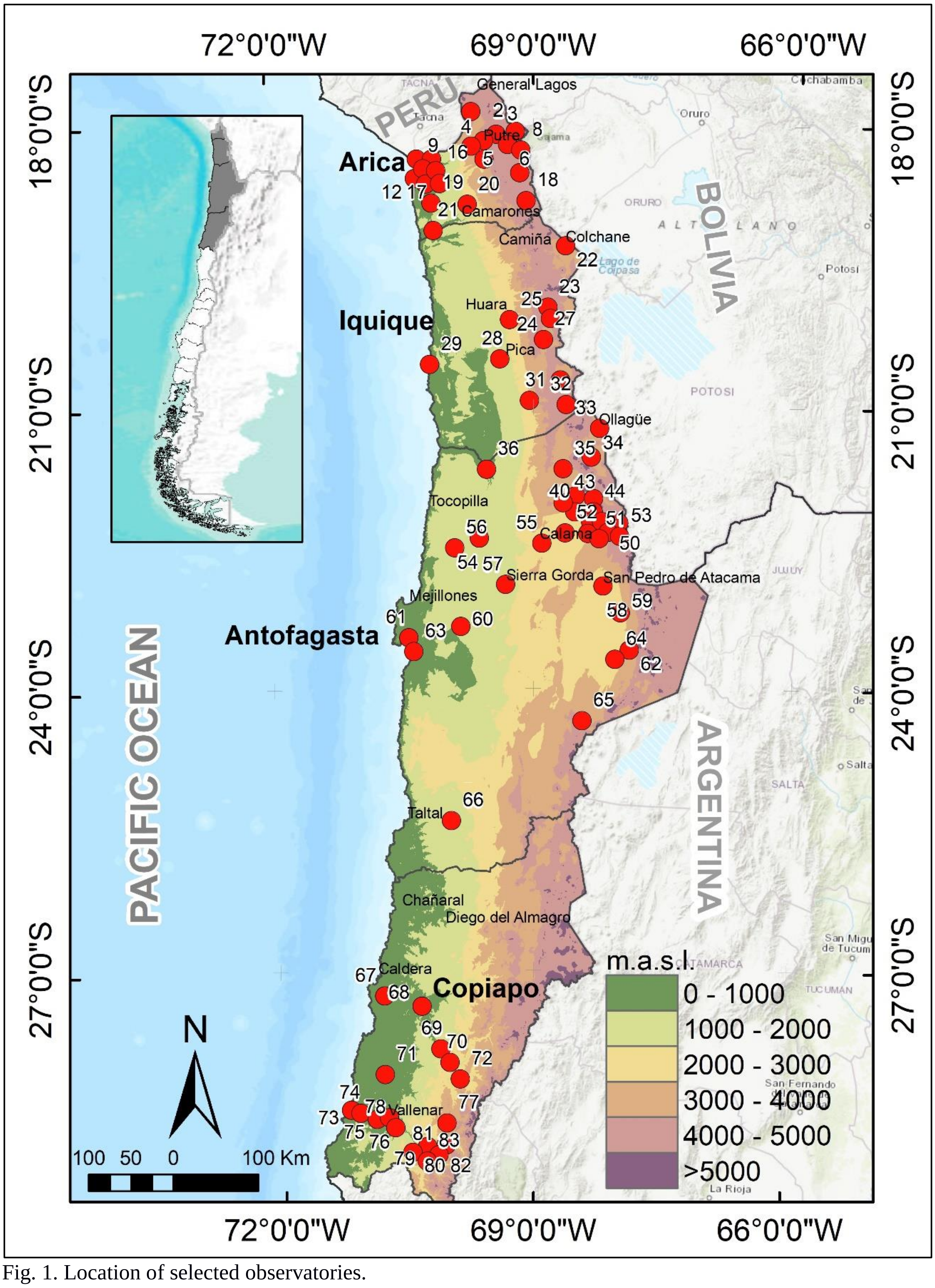

Fig. 1. Location of selected observatories.

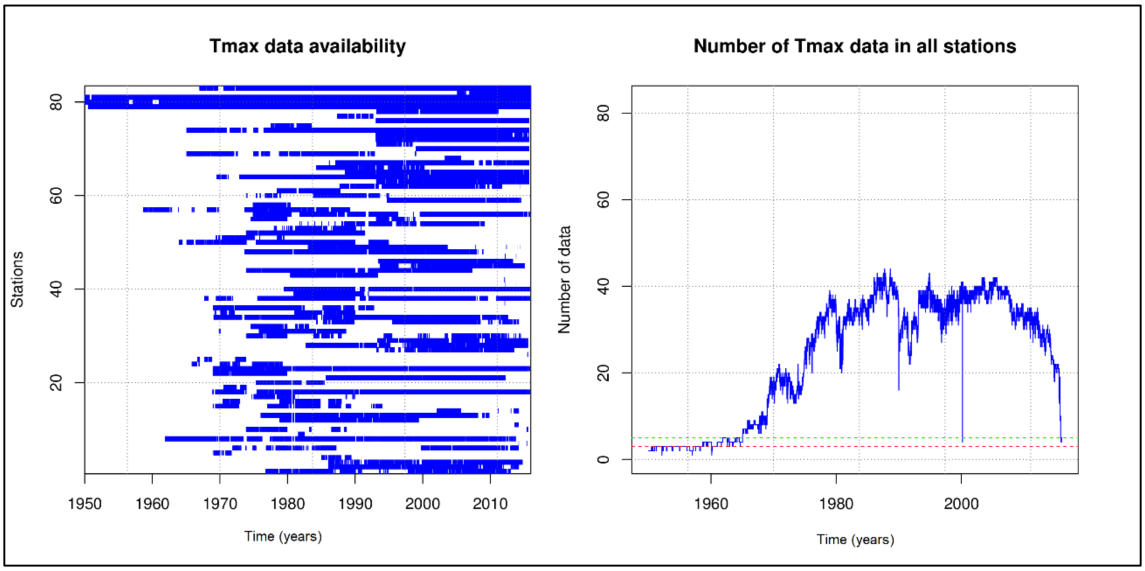

Fig. 2. Data availability in the 77 series (a) and overall (b). Dashed green and red lines show desirable and minimum availability thresholds for a reliable homogenization and quality control of the series.

2.1. Homogenization and quality control

The quality control and homogenization was performed by means of the R package Climatol version 3.0 (Guijarro 2016). The procedure consists in estimating all data (whether measured or missing) in every series by a weighted or plain average of the closest available data, in normalized form, at each time step. Normalization allows to minimize problems due to spatial variability in means and standard deviations caused by different elevations and other topographic factors. A first problem is the difficulty of computing means and standard deviations for the whole period of study when series are not complete, which is often the case. Therefore, series are first normalized with their available data; missing data are estimated after this first normalization, and new means and standard deviations are then computed for the completed series. This process is repeated until the maximum difference in means from the previous iteration is lower than half the resolution of the data (0.05 °C in our case), because any further improvement would not modify the rounded results. Quality control is performed along these iterations by comparing the observed and the estimated values, both in normalized form, and deleting those differing more than a prescribed number of standard deviations. By default, the rejection threshold is set to five standard deviations, which may be appropriate for monthly temperatures, but not for other variables or time resolutions. Therefore, the user of the package is advised to set this threshold subjectively after looking at the histogram of anomalies of an exploratory run (Guijarro 2018). Many users would prefer to use an objective criterion to set the threshold, such as choosing a level of significance, but this is also a subjective decision, and significant levels would differ depending on the studied climatic element, time resolution and cross-correlation between the series. All this complexity is avoided by letting the users decide which parts of the tails of the anomalies distribution should be rejected and allowing them to choose different upper and lower thresholds when the probability distribution of the variable shows a clear skewness.

Homogeneity is then tested in each observed series by means of the Standard Normal Homogeneity Test (SNHT, Alexandersson 1986), which computes a test for differences of means before and after every point of a series and reports the maximum value reached and its location. This test is applied on the differences between the observed series and its estimated series, previously calculated from data at nearby stations, both in normalized form.

The most inhomogeneous series are then split at the points where SNHT reaches their maximum values, transferring data to new "daughter" series which are assigned the same coordinates as their original series. No series is split when a reference series has also been split, and hence the homogenization is also carried out through an iterative process until no SNHT value is higher than a pre-set threshold. Note that after every splitting iteration all series means and standard deviations must be recalculated and new quality control performed. Therefore, this very simple methodology increases its complexity through different stages of nested iterative processes, which are performed in an automated way. In a first stage, SNHT is applied on stepped overlapping temporal windows in order to avoid possible masking effects of more than one big inhomogeneity in the series. Then, SNHT is computed on the whole series, and finally, a third stage is devoted to the last in-filling of all missing data in all series (original and derived). Up to 10 reference data were averaged in the first two stages, and only 4 in the last one, this time weighting them by an inverse function of distance.

Thresholds for outlier rejection and inhomogeneity detection vary depending on the studied climatic element, the time resolution of the series and the station density combined with the spatial climate variability. Therefore, although a default value of SNHT=25 is set in the software, the user can choose appropriate thresholds by inspecting histograms yielded in a first exploratory application of the package. The high variability of daily series lowers the power of detection of inhomogeneities (Szentimrey 2013), and therefore it is advised to perform this process on the monthly aggregates, as was done in our study. Then, the list of the dates of the detected break-points was used to adjust the daily series by splitting them at those time steps and reconstructing complete series from every homogeneous subperiod by the missing data in-filling procedure. These analysis were applied to the period 1950-2015, but as the station density in the first years was very low, only results for 1966-2015 were retained for the rest of the study.

2.2 Temperature indices

All the temperature indices were calculated from the homogenized daily series. In a first place, the annual values of maximum and minimum temperatures for each observatory was determined. After that, the mean value for every year was calculated, and then the anomalies were computed to define TXMean and TNMean, defined as the indicators of absolute extreme temperature anomalies evolution for the period 1966-2015.
In a second place, we considered a series of indices defined by Frich et al. (2002) that later became known as the ETCCDI indices, and which were based on the indices proposed that same year by the European Climate Assessment (ECA) (Klein Tank et al. 2002) to analyse trends in the second half of the 20th century. These ETCCDI indices were selected in order to handle a wide variety of climates. For this study, a selection of 14 of the 29 ETCCDI indices will be applied (Table 1). These indices are applicable to most global climates and can be compared between different regions in the world.

Table 1: Extreme temperature indices used. Source: Extracted and modified from Klein Tank et al. (2002).

Index	Name	Definition	Units
TXx	T_{max} Max	Monthly maximum value of daily maximum temperature	°C
TNx	T_{min} Max	Monthly maximum value of daily minimum temperature	°C
TXn	T_{max} Min	Monthly minimum value of daily maximum temperature	°C
TNn	T_{min} Min	Monthly minimum value of daily minimum temperature	°C
TN10p	Cold nights	Annual count of daily minimum temperature < 10th percentile	days
TX10p	Cold days	Annual count of daily maximum temperature < 10th percentile	days
TN90p	Warm nights	Annual count of daily minimum temperature > 90th percentile	days
TX90p	Warm days	Annual count of daily maximum temperature > 90th percentile	days
DTR	Diurnal temperature range	Monthly mean difference between daily maximum and minimum temperature	°C
FD0	Frost days	Annual account of daily minimum temperature < 0º C	days
SU25	Summer days	Annual count of daily maximum temperature > 25º C	days
TR20	Tropical nights	Annual count of daily minimum temperature >20°C	days
WSDI	Warm spell duration indicator	Annual account of at least six consecutive days of maximum temperature > 90th percentile	days
CSDI	Cold spell duration indicator	Annual account of at least six consecutive days of minimum temperature < 10th percentile	days

Some of these indices (TXx, TNx, TXn, and TNn) measure the maximum or minimum daily temperature on an annual basis. Doing this, we are able to evaluate the evolution of the maximum and minimum temperatures both in the cold and warm season. Other indices allow calculations of the number of days a year when specific fixed value thresholds are exceeded or refer to a base climatic period. Nevertheless, indices based on percentile thresholds (TN10p, TX10p, TN90p, TX90p, WSDI and CSDI) are preferable when making spatial comparisons of extremes due to possible differences in temperature distribution samples when using day-count indices with fixed thresholds across large areas. For example, sustained heat in mid-latitude climates could be well indicated by counting the number of days with a minimum temperature above 20°C (TR20); on the contrary, in low latitudes, where minimum temperatures on most summer nights are above this threshold, the variability in the annual number of nights with temperatures above 20°C is determined by the conditions in spring and autumn. Furthermore, an index such as the number of summer days with maximum temperatures over 25°C (SU25) can indicate abnormally warm

conditions in normally temperate climates, where the average maximum summer temperature is around 18°C (Zhang et al. 2011).
The determination of the extreme values was performed with R, and the scripts used are available as supplementary material.
In order to determine the possible existence of temporal trends in the monthly maxima, minima, and extreme indices, the series of average monthly and extreme daily temperatures are analysed, and their statistical significance is determined by the Mann-Kendall non-parametric test (MK) (Mann 1945; Kendall 1962). The test has been widely used in the analysis of hydro-meteorological time series (Cai et al. 2017; Caloiero et al. 2017; Liang et al. 2017; Tao et al. 2014). The MK statistic is obtained as follows:

$$S = \sum_{i=1}^{n-1} \sum_{j=i+1}^{n} \mathrm{sgn}(x_j - x_i) \quad (1)$$

$$\left(x_j - x_i\right) = z \quad (2)$$

$$\mathrm{sgn}(z) = \begin{cases} 1 \text{ if } (z) \geq 0 \\ 0 \text{ if } (z) = 0 \\ -1 \text{ if } (z) \leq 0 \end{cases} \quad (3)$$

Where n is the dimension of the series and x_j and x_i are the annual values, respectively, in the years j and i, with j > i. For n > 10, given that x_i is an independent and randomly ordered series, the statistic S follows a normal distribution whose mean is equal to 0, and the variance is provided by:

$$\mathrm{Var}(S) = [n(n-1)(2n+5) \sum_{i=1}^{n} t_i i(i-1)(2i+5)]/18 \quad (4)$$

Where t_i represents a margin of error of i.
The standardized statistical test Z_{MK} follows a standard normal distribution, and is represented by:

$$Z_{MK} = \begin{cases} \frac{S-1}{\sqrt{\mathrm{Var}(S)}} \text{ if } S > 0 \\ 0 \text{ if } S = 0 \\ \frac{S+1}{\sqrt{\mathrm{Var}(S)}} \text{ if } S < 0 \end{cases} \quad (5)$$

Using a two-tailed test, if Z_{MK} is greater than $Z_{(\alpha/2)}$, with a significance level α, then it is possible to reject the null hypothesis and the trend can be considered significant. At the 10% significance level, the null hypothesis of no trend is rejected if |Z|>1.645.
To estimate the magnitude of the slope we use the nonparametric Sen slope estimator (Sen 1968). This approach involves computing the slopes for all temporally ordered pairs of data points and then calculating the median of these slopes as an estimate of the overall slope (Salmi et al. 2002). Since Sen's slope is not greatly affected by single data errors or outliers and missing values are also allowed, it is more rigorous than the commonly used regression slopes and thus provides a realistic measure of the trends in the time series. Sen's method can be used in cases where the trend can be assumed to be linear. This means that f(t) is equal to

$$f(t) = Qt + B \quad (6)$$

where f(t) is a continuous monotonic increasing or decreasing function of time, Q is the slope and B is a constant. To obtain the slope estimate Q in Eq. (6) we first calculate the slopes of all data value pairs

$$Q_i = \frac{x_j - x_k}{j-k} \quad (7)$$

in which j>k. A positive value of Qi indicates an increasing trend whereas a negative value indicates a decreasing trend. If there are n values x_j in the time series we get as many as $N = n(n-l)/2$ slope estimates Q_i. The Sen's estimator of slope is the median of these N values of Q_i. The N values of Q_i are ranked from the smallest to the largest and the Sen's estimator is

$$Q = \begin{cases} Q_{[(N+1)/2]} \; if\ N\ is\ odd \\ \frac{Q_{\left[\frac{N}{2}\right]} + Q_{\left[\frac{(N+2)}{2}\right]}}{2} \; if\ N\ is\ even \end{cases} \quad (8)$$

The Q sign denotes data trend reflection, while its value indicates the steepness of the trend. To determine whether the median slope is statistically different from zero, one should obtain the confidence interval of Q at specific probability. The confidence interval about the time slope can be computed as follows:

$$C_{\alpha} = Z_{1-\alpha/2}\sqrt{Var(S)} \quad (9)$$

where Var(S) is same defined as the variance in MK test and $Z_{1-\alpha/2}$ is obtained from the standard normal distribution table. In this study, we calculated the confidence interval at $\alpha = 0.1$.
Then $M_1 = (N - C_{\alpha})/2$ and $M_2 = (N + C_{\alpha})/2$ are computed. The lower and upper limits of the confidence interval, Q_{min} and Q_{max}, are the M_1th largest and the (M_2 + 1) the largest of the N ordered slope estimates Q_i. The slope Q is statistically different from zero if the two limits (Q_{min} and Q_{max}) have the same sign. To obtain an estimate of B in Eq. (6) the n values of differences x_i-Q_{ti} are calculated. Their median of these values gives an estimate of B. Estimates for the constant B of lines of the 90% confidence interval are calculated by a similar procedure (Salmi et al. 2002).

3. Results and discussion

3.1. Homogenization and quality control

Figures 3a and 3b show the histograms of final SNHT values after the homogenization of the monthly averages of maximum temperatures over SNHT=50 and of daily maximum temperature anomalies. Outliers of more than 10 standard deviations (in red) were deleted and in-filled at the end of the process. Decisions about outlier rejections and shifts in the mean corrections are always driven by choosing a balance between detection failures (type I errors) and false alarms (type II errors). The threshold for SNHT (50) is a conservative figure trying to avoid as many false detections as possible while disregarding a moderate number of small shifts in the mean. As to the threshold chosen for outlier rejection, 10 standard deviations may seem a very high figure, but daily data variability in an area of complex orography is very high, and false rejections should be mostly avoided when series will be used for extreme values analysis. Ideally, both rejected data and detected shifts should be confirmed with the help of metadata, but these are generally very scarce, if not absent. Even with this high threshold, some rejected data could correspond to real extreme values, and should be reinstated in the series if its validity is confirmed, but it is better to remove them in the homogenization process to avoid local rare phenomena to be taken as references to in-fill missing data of other series in the data-set.
Figure 4 shows an example of detection of a shift in the mean (with SNHT=62) in a monthly series and the adjustment of its corresponding daily series. A complete reconstruction of the two homogeneous subperiods are performed, with correction terms of around 2 °C, but with a clear seasonal variation.
Monthly aggregates of the maximum temperatures appeared more homogeneous (31 break-points detected) than their minimum monthly aggregates (58 break-points), and 22 and 5 outliers of more than 10 standard deviations were deleted in maximum and minimum temperatures, respectively.
Series adjusted backwards from the last homogeneous subperiods were used for the subsequent analysis of the variability of temperature in the region.

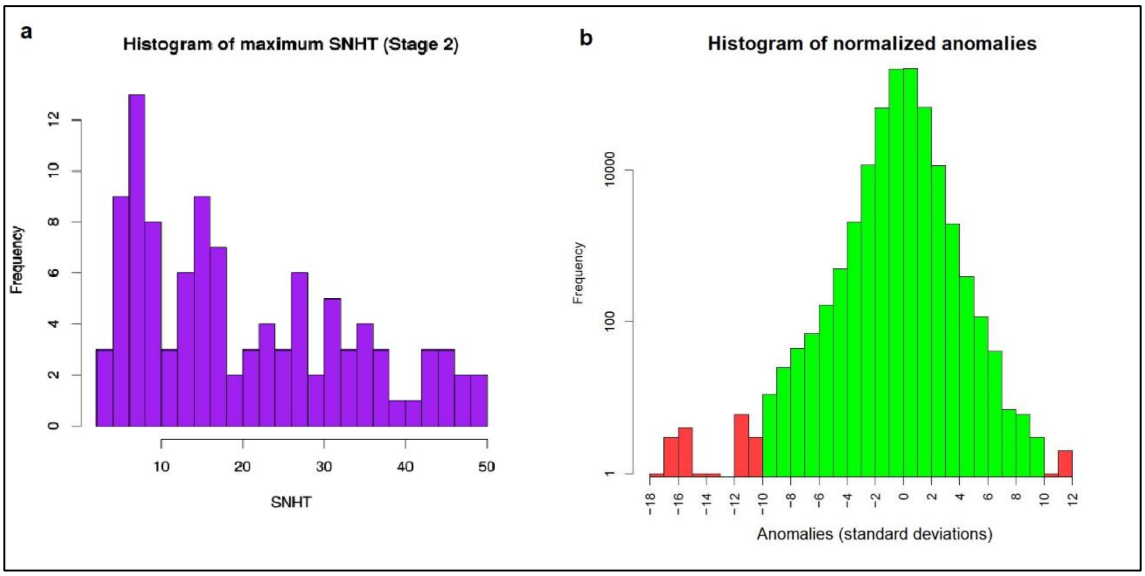

Fig. 3. a) Histogram of maximum SNHT values in all monthly means of maximum temperature series after homogenizing those exceeding SNHT=50. b) Histogram of daily maximum temperature anomalies; in red, rejected data with anomalies higher than 10 standard deviations.

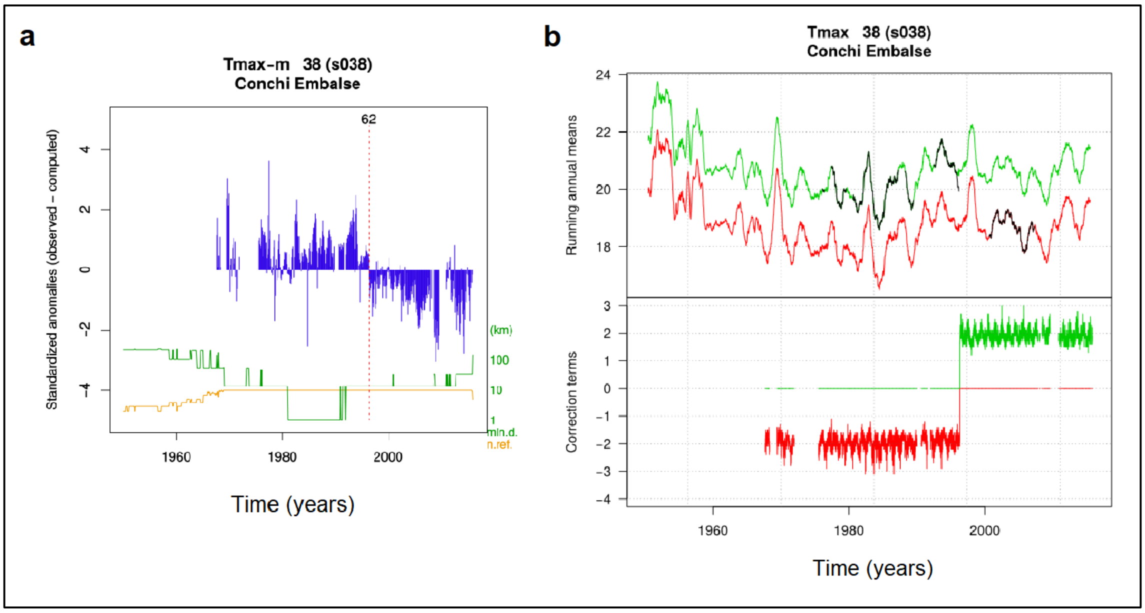

Fig. 4. a) Example of detection of a shift in the mean with SNHT=62. Distances to the closest data at each time step and number of references used are shown in green and orange respectively. b) Adjustment of the detected inhomogeneity: complete reconstruction of the two homogeneous subperiods are shown in red and green (top), with observed values in black. (Running annual means are plotted to reduce the noise of the figure, and hence observed data are plotted only when no missing data are present). The bottom graphs show the correction terms applied to every data in both subseries. Note that due to the reduced number of available data, only values from 1966 are used in this study.

3.2. Temporal variability of trends in TXMean and TNMean

TXMean and TNMean were calculated, and their temporal evolution between 1966 and 2015 are shown in Figure 5. The statistics of trend based on the Sen slope estimate applied to the annual time series indicate asymmetric trends of maximum temperature (TXMean) and minimum temperature (TNMean). In the first case, non-significant positive trends were identified, with a Sen slope estimate of 0.007 (0.007ºC/year), meanwhile minimum temperature indicator showed a Sen slope estimate of 0.071 (0.071ºC/year) with a high significance level (>99.9%). These results agree with those identified in other studies that claim that the identified rise of mean temperatures was due to rise in minimum temperatures, and not so evident rise of maximum temperatures (IPCC 2013; Vose et al. 2005; Vuille et al. 2015).

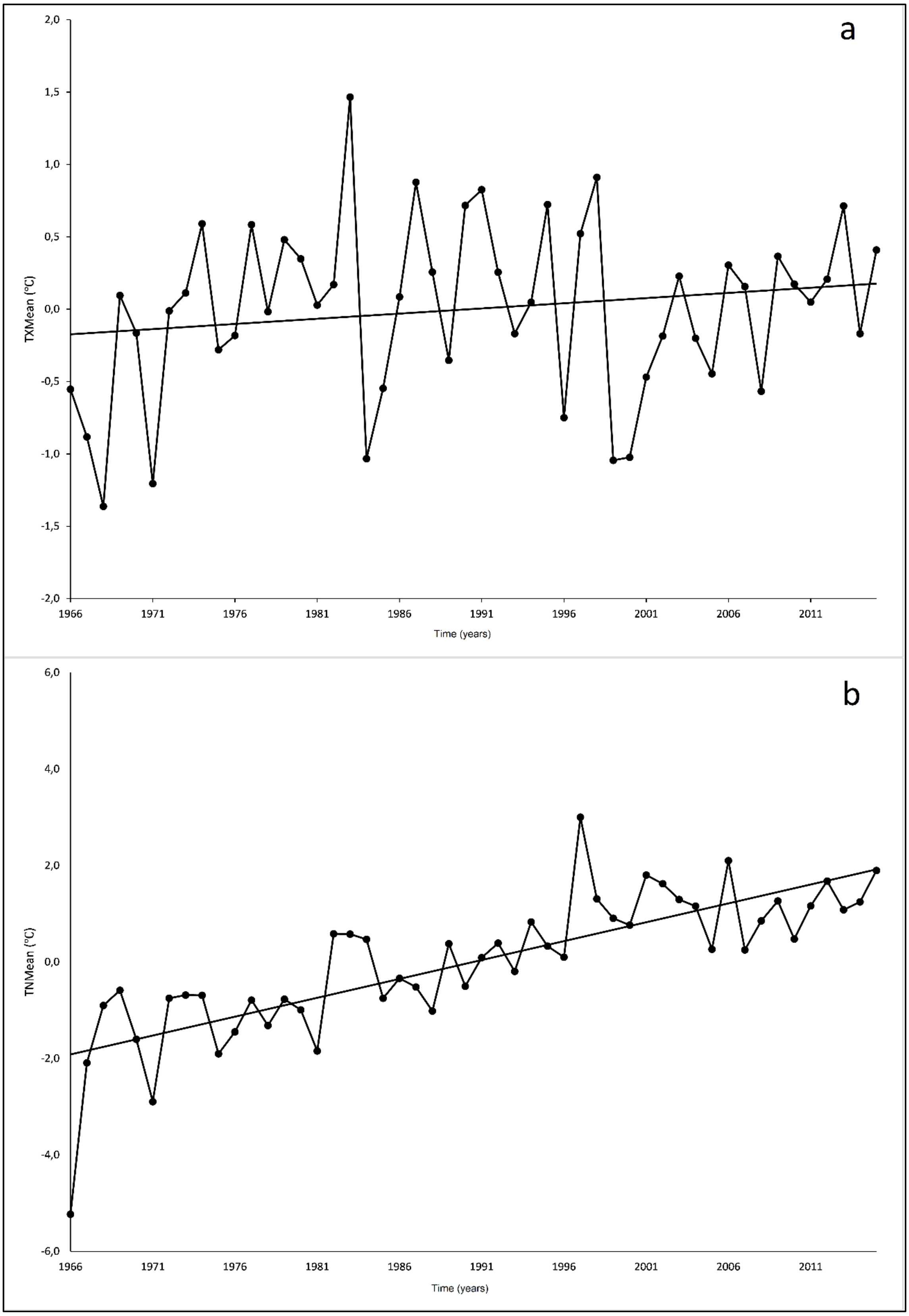

Fig. 5. Time series and trend of a) TXMean and b) TNMean anomalies

3.3. Spatial behaviour of extreme temperatures indices

To provide better understanding of trends in extreme temperature indices, their statistical significance is assessed at the 90% confidence level employing the MK trend test. Sign and significance of the trends are shown in Figure 6. The percentage of the absolute minima (TNn) show the highest number of positive and significant trends (87%), followed by the TXn index (57%). This result agrees with those identified by Tao et al. (2014) in other regions in the world. In contrast, relative indices based on minimum temperatures (TN10p and TN90p) show negative and significative signs or even not significative trends. Absolute maximum indices (TXx and TXn) show positive and significant trends in an important number of stations, but more evident in lower maxima (35% and 57% respectively). Meanwhile, the highest minima TNx show a high number of negative and significant trends (65%) and only a few stations with positive trends (4%). Relative indices based on maximum temperatures (TX10p and TX90p) show different: while lower maximum temperatures show 70% of negative trends (TX10p), higher maximum temperatures (TX90p) show 40% of positive and significative trends and a 14% of negative trends. DTR shows almost 20% of positive trends, which means that in these stations maximum temperatures rose significantly more than minimum temperatures, since minimum values of minimum temperatures showed a significant increase in more than 85% of the stations. Frost days (FD0) showed significative negative trends in 28% of stations, and positive and significative trends in 16% stations. SU25 shows 40% of positive and significative trends, and 9% of negative and significative trends. Tropical nights (TR20) shows a significant negative trend un 4% of the stations, and no significant trend is recorded at any stations for WSDI, which means that sustained warm episodes have experienced no changes. At least, CSDI, cold sustained events, shows negative and significant trends in 82% of the stations, and no positive trends.

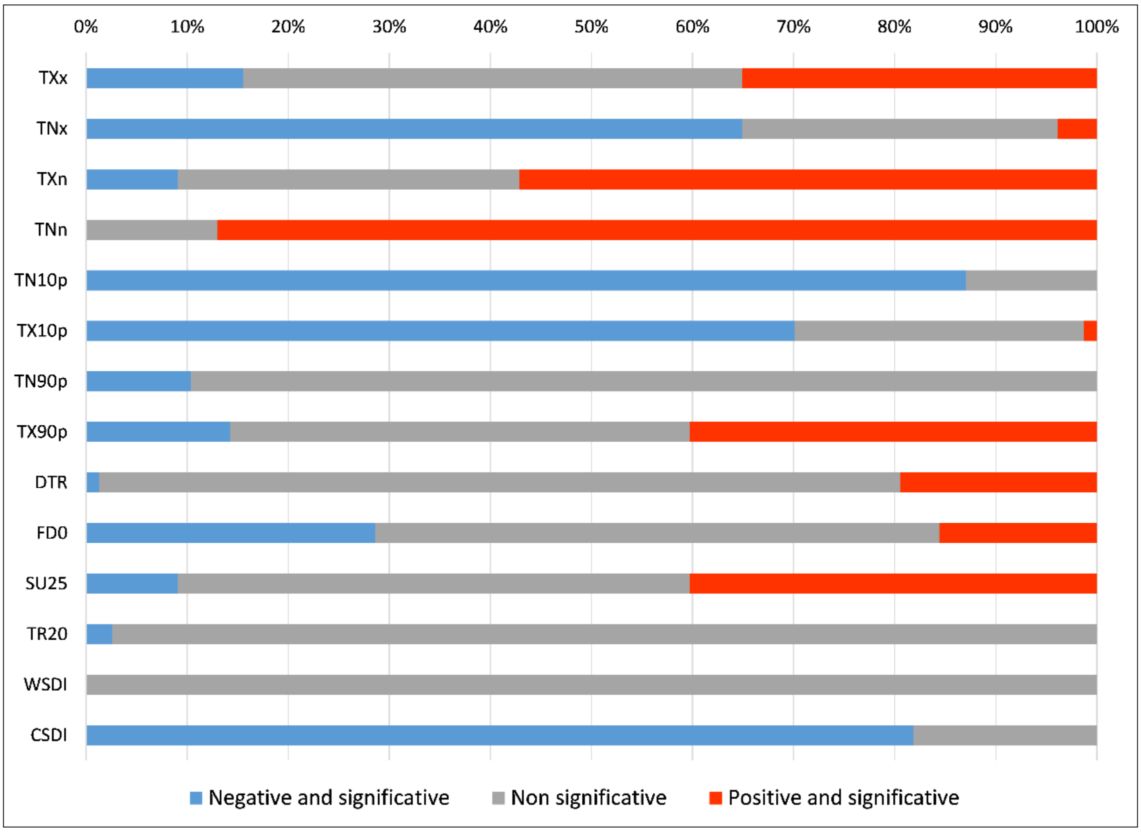

Fig. 6. Trends of the temperature indices (% of stations): TXx (Tmax Max), TNx (Tmin Max), TXn (Tmax Min), TNn (Tmin Min), TN10p (cold nights), TX10p (cold days), TN90p (warm nights), TX90p (warm days), DTR (diurnal temperature range), FD0 (frost days), SU25 (summer days), TR20 (tropical nights), WSDI (warm spell duration indicator), CSDI (cold spell duration indicator)

Figure 7 shows the spatial distribution of the identified trends of extreme temperatures. The indices TXx, TNx, TXn and TNn, are shown in Figures 7a, 7b, 7c and 7d, respectively, and represent variations on punctual intensity of daily extremes. The most evident warming according to the maximum temperatures is seen in the southern area while referring to the TXx index meaning that highest maximum temperatures are more sensitive to global warming in this area, while the TXn index was more obvious in the area north of to the Tropic of Capricorn. Both indices show different trends, TXx was positive and significant at 24 stations, negative and significant trends at 11 stations, and the rest with no significant trends; TXn showed 44 positive and significant trends and 7 negative and significant trends. According to TXx, station 67 showed a positive significant trend of +1.08ºC /decade, the highest recorded value for this index, and TXn shows a +1.15ºC /decade in station 49. An important observation was that intense negative significant trends have been recorded at stations 73 and 62, reaching -1.29 and -1.28ºC / decade respectively for TXn. The minimum temperatures show a more homogeneous behaviour represented here by TNx and TNn, where there was a general decline in the TNx index but a clear increase in TNn for the whole area was evident. Maximum values of minimum temperatures have decreased in the inter-tropical area of Northern Chile, even reaching on average -1.67ºC / decade at station 31. The lowest minimum temperatures have increased 0.73ºC / decade by mean, reaching 1.85ºC / decade at station 34. But the highest warming values of the 4 absolute indices was reached in the TNn index, where 21 stations registered trends higher than +1ºC / decade, reaching +1.85ºC / decade at station 34, and being located the most of these stations in the northern area of the study region. TNn does not show any negative and significant trends. These results agree with those presented in the IPCC (2013), which refer to the observed warming in mean temperatures was mainly due to an increase in minimum temperatures. They also agree with other close regions (Seiler et al. 2013; Vicente-Serrano et al. 2017; Burger et al. 2018). The recent slowdown in the warming rhythms is not well evidenced, possibly due to the fact that most of the study period was limited to the 20th Century.

When we looked at the extreme percentile-based indices (Figures 7e, 7f, 7g and 7h), the trend analysis of TN10p, TX10p, TN90p and TX90p show more negative trends for the first three indices. In fact, TN10p shows a significant negative trend at 73 stations, with a rate of -16.25 days / decade in station 36, and TX10p shows negative trends at 60 stations, with a rate reaching -15 days / decade at stations 15 and 20, as the most evident changes. TN90p index only shows two significant and positive trends, but 54 negative trends, with a highest intensity of -5.63 days / decade. On the other hand, TX90p presents 30 positive trends and 10 negative trends, values ranging from -6.14 to 10 days / decade. There are positive trends found in the whole study area, but the negative trends seem to be located specifically in the northern area. These results agree with the general warming tendencies identified for neighbour regions (Vuille et al. 2015).

The analysis of the DTR index (Figure 7i) shows 15 stations with a positive significant trend and only one with a negative trend. The positive trends are located from the centre of the study area southward, with a maximum rate of +0.5ºC / decade. This trend reflects the similar findings previously detected in the literature. In fact, some studies found significant decreasing DTR trends, because of a faster warming in minimum temperatures than in maximum temperatures, while other analyses of DTR fluctuations at a global scale are evidenced by a large increasing trend caused by an opposite behaviour (Vose et al. 2005; Guan et al. 2015). For example, frost days (FD0) show 22 stations with negative and significant trends, mainly located in the central area, around the Tropic of Capricorn (Figure 7j), and 11 stations with positive and significant trends, showing rates ranging from -15.56 days / decade to +15 days / decade. Major positive trends can be identified in 29 stations for summer days (SU 25, Figure 7k), with intensities reaching +15.7 days / decade, but in the North, a negative and non-significant trend dominates, with rates of -16.7 days / decade. These results agree with Falvey and Garreaud (2009), and with Burger et al. (2018), where some cooling trends were identified for some mean monthly temperatures in the continent. The tropical nights index TR20 (Figure 7l) shows a high number of non-significant trends because of the lack of days which accomplished this condition. Only two stations recorded significant negative trends, -3.8 and -4.2 days / decade on the northern coast of the study area, agreeing with other studies identifying the tropical coast of South America was conforming to a general trend of slowing down of the warming rhythms (Vuille et al. 2015).

The WSD Index denotes an increasing trend at 23 stations (Figure 7m), with a maximum of +5.13 days / decade detected for station 82, and it identifies 10 negative trends, with a loss of +4.5 days / decade, mainly in the North of the study area. This agrees with similar trends detected in Parak et al. (2015) for high elevated areas. On the contrary, the results obtained for the cold spell duration indicator CSDI (Figure 7n) shows a very evident negative behaviour for 40 stations, located in the centre and a major part of the study area, with rates reaching -5.9 days / decade, disaccording with the results of Rahimi and Hejabi (2017), where no significant trends of this index where identified.

The trend analysis of extreme temperature indices in Northern Chile show an evident increase in intensity of warmer extremes but not so evident in its frequency and a less notable increasing trend or more balanced rates for the colder extremes. These results partially agree with those presented in the most recent IPCC analysis (IPCC 2013), where a major part of land areas are likely to have experienced decreases in cold extreme indices and increases in warm extreme indices. When compared to more regional studies, the trends identified agree with those found in neighbour regions (Thibeault et al. 2010, Seiler et al. 2013).

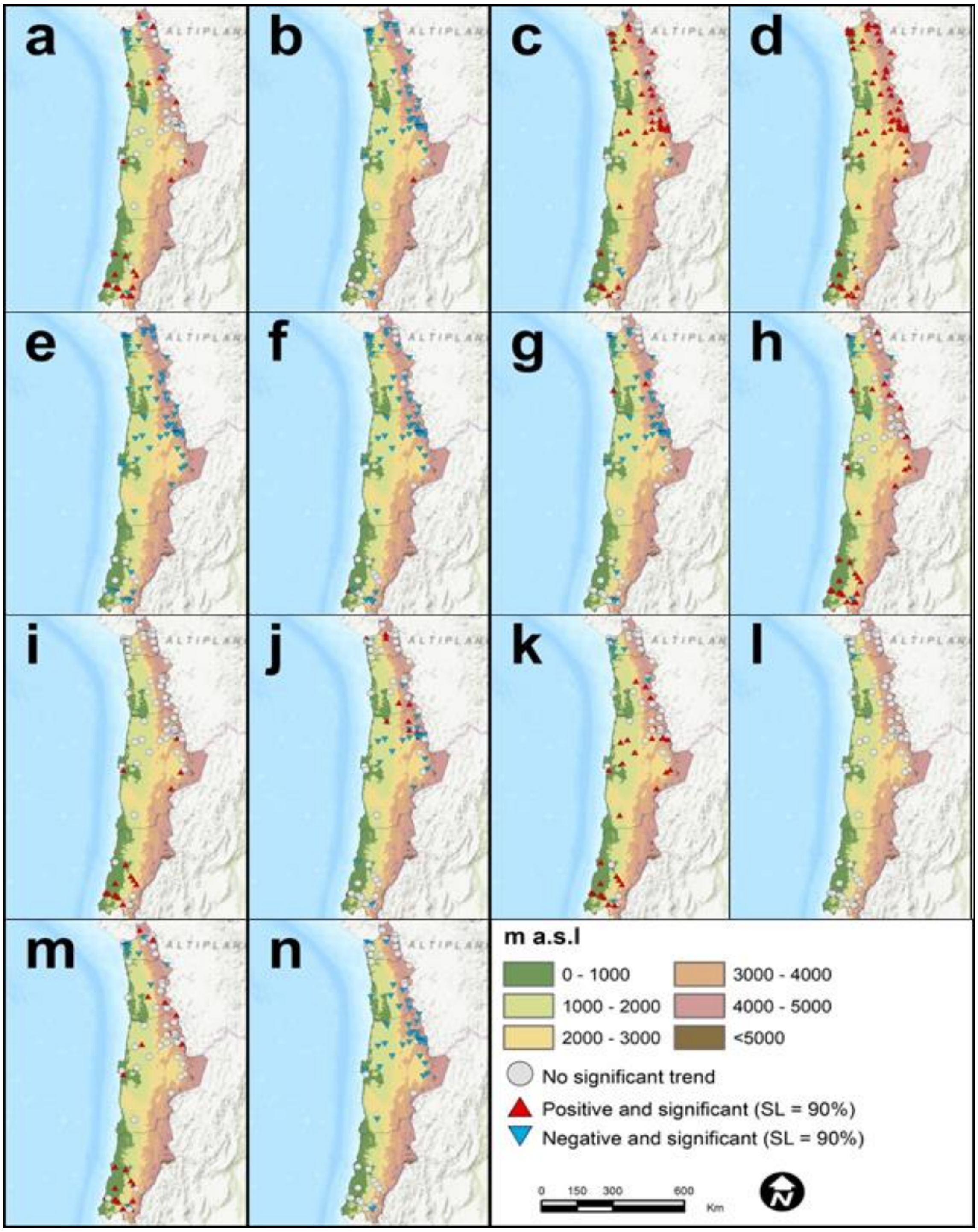

Fig. 7. Spatial distribution of the different extreme temperatures indices significant trends: a. TXx, b. TNx, c. TXn, d. TNn, e. TN10p, f. TX10p, g. TN90p, h. TX90p, i. DTR, j. FD0, k. SU25, l. TR20, m. WSDI and n. CSDI (significance level: 90%)

Table 2 shows the correlation between the 14 indices used in this study. TXx is significantly correlated to all indices except for TN90p, FD0 and WSDI. The highest r Pearson's values are found in TX10p (0.75), TX90p (0.90) and SU25 (0.64), being those three indices directly related to the behaviour of the highest maxima. Negative and significant correlations are found with TXn (-0.39) and TNn (-0.23). This could explain the positive trends detected for some stations for the DTR index. TNx index shows high positive and significative correlations with TN10p (0.78) and CSDI (0.70), explained because those three indices are based on the maximum values of minimum temperatures. TNx show high negative and significative correlations with TXn (-0.60) and TNn (-0.83). The trends shown in the minimum values of maxima and minimum values of minima explains this change in the relationship. TXn index is positively correlated with TNn (0.57), showing a similar evolution of lowest minimum and maximum temperatures. It is negatively correlated with TN10p (-0.57), TX10p (-0.55) and CSDI (-0.60). TNn is significant and negatively correlated with TN10p (-0.70) and with CSDI (-0.65). This is explained because of the rise of lowest minimum temperatures, and TN10p and CSDI are showing the regression of the persistence of cold events. TN10p is highly correlated to TX10p (0.51), TX90p (0.55) and CSDI (0.90), showing the general trend into more warm climate. TX10p shows a high positive correlation with TX90p (0.71), SU25 (0.70) and TR20 (0.57), all indices linked to warming trends. TX90p is highly correlated to SU25 (0.60), both linked to the behaviour of highest maximum temperatures. Finally, SU25 is positively correlated to TR20 (0.51), explaining the relationship between this two indices, if maximum temperatures are higher, minimum temperatures do not fall as much as they tend to do.

Table 2. R-Pearson's correlation coefficient between indices. The significant correlations ($p<0.1$) are coloured in blue: TXx (Tmax Max), TNx (Tmin Max), TXn (Tmax Min), TNn (Tmin Min), TN10p (cold nights), TX10p (cold days), TN90p (warm nights), TX90p (warm days), DTR (diurnal temperature range), FD0 (frost days), SU25 (summer days), TR20 (tropical nights), CSDI (cold spell duration indicator)

	TXx	TNx	TXn	TNn	TN10p	TX10p	TN90p	TX90p	DTR	FD0	SU25	TR20
CSDI	0.35	0.70	-0.60	-0.65	0.90	0.39	0.31	0.39	0.28	-0.09	0.20	-0,04
TR20	0.42	-0.09	-0.14	0.11	-0.01	0.57	-0.08	0.41	0.12	-0.03	0.51	
SU25	0.64	0.22	-0.22	-0.06	0.29	0.70	0.02	0.64	0.46	-0.16		
FD0	-0.07	-0.24	0.15	0.15	-0.15	-0.12	-0.21	-0.03	0.07			
DTR	0.30	0.15	-0.11	-0.13	0.33	0.28	0.03	0.44				
TX90p	0.90	0.40	-0.38	-0.21	0.55	0.71	0.12					
TN90p	0.10	0.48	-0.17	-0.36	0.36	0.05						
TX10p	0.75	0.34	-0.55	-0.26	0.51							
TN10p	0.51	0.78	-0.57	-0.70								
TNn	-0.23	-0.83	0.57									
TXn	-0.39	-0.60										
TNx	0.39											

Figure 8 shows the correlation of the trend in each meteorological station with each other for each index calculated in this study. Blue tones show positive correlations of each index for each meteorological station, ordered by latitude. Red colours show a negative correlation, expressing changes in the trends between stations. TNx, TNn, TN10p, TX10p, TN90p, DTR and CSDI indices show homogenous behaviours. TR20 shows many null correlations, linked to the stations with no days with minimum temperature over 20ºC in the whole study period. TXx, TXn and TX90p indices show some shifts in the trends in the stations located between 20ºS and 22ºS, identifying a region with a special behaviour of maximum temperatures. FD0 show also some shifts in the trends, without any clear spatial distribution pattern, more linked to the location of the observatories in high elevated areas or close to the coast. SU25 index shows clear changes also in the stations between 21ºS and 23ºS, determining that between these latitudes, there is not a significant number of stations located at high elevated areas, so maximum daily temperatures are able to rise to higher values. WSDI index shows low shifts in the northern part of the study area.

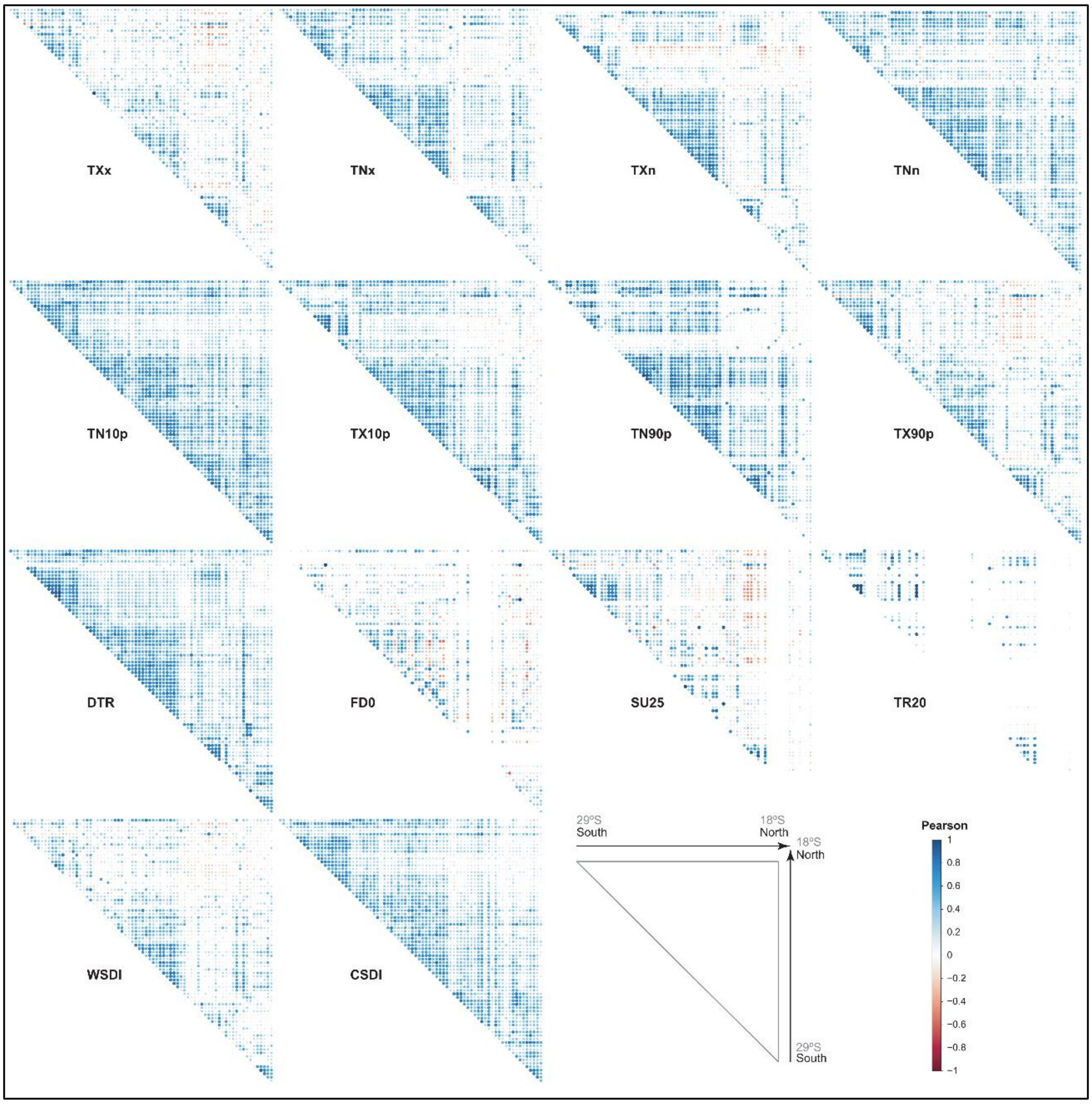

Fig. 8. Correlation between meteorological stations for each index: TXx (Tmax Max), TNx (Tmin Max), TXn (Tmax Min), TNn (Tmin Min), TN10p (cold nights), TX10p (cold days), TN90p (warm nights), TX90p (warm days), DTR (diurnal temperature range), FD0 (frost days), SU25 (summer days), TR20 (tropical nights), WSDI (warm spell duration indicator), CSDI (cold spell duration indicator)

3.4. The relationship between temporal trends of indices with elevation and latitude

The different extreme temperature indices show widely varying R-Pearson's correlations with altitude and latitude (Table 3).

Table 3. R-Pearson's correlation coefficient between indices and altitude and latitude. The significant correlations ($p<0.1$) are coloured in blue: TXx (Tmax Max), TNx (Tmin Max), TXn (Tmax Min), TNn (Tmin Min), TN10p (cold nights), TX10p (cold days), TN90p (warm nights), TX90p (warm days), DTR (diurnal temperature range), FD0 (frost days), SU25 (summer days), TR20 (tropical nights), WSDI (warm spell duration indicator), CSDI (cold spell duration indicator)

Index	Altitude	Latitude
TXx	-0.08	-0.55
TNx	-0.38	-0.32
TXn	0.15	0.11
TNn	0.40	0.21
TN10p	-0.32	-0.45
TX10p	-0.03	-0.40
TN90p	-0.20	-0.23

TX90p	-0.14	-0.65
DTR	-0.30	-0.61
FD0	-0.01	0.07
SU25	-0.06	-0.56
TR20	0.25	-0.09
WSDI	0.00	-0.54
CSDI	-0.26	-0.25

Figure 9 shows the temporal trends of extreme temperature indices and the elevations of the selected observatories from sea level (in meters). Some indices do not show any relationship with elevation, as can be seen for TXx and TXn (Figures 9a and 9c), but others such as minimum temperatures do show a clear relationship with TNx and TNn, with r Pearson coefficients of -0.38 and 0.40 respectively (Figures 9b and 9d). The TNx index shows more intense negative rates in higher elevated areas, over 2,500 m.a.s.l., and TNn show higher rates over 2,000 m.a.s.l. This agrees with similar trends observed in Vuille et al. (2015). In general, frequency variations of TX10p and TX90p were found to be lower than that of TN10p and TN90p, which were also correlated with the elevation (Figures 9e, 9f, 9g and 9h), and which was in agreement with the findings at Berman et al. (2013) and at Kattel and Yao (2018). Most stations had increasing trends of DTR (Figure 9i), with a significant r Pearson correlation of -0.30. This was likely due to the increasing trend of maximum temperatures, being sharper than that of minimum temperatures. At lower elevations, the effect of cloud cover on temperature pushes the trend of DTR towards positive values. FD0 index do not show a significant trend, observatories in high and low altitudes have positive and negative trends, so there is no evidence of a most sharply decreasing frequency of frost days at higher elevations (Figure 9j). Figure 9k shows the SU25 index, which has a generally increasing trend at most stations, however a few stations had a decreasing trend, such as those at the higher elevations, which tended to have a lower increase in SU25. Some of the negative trends of TR20, with a significant correlation of 0.25, are located in high elevated areas (Figure 9l), which agrees with Bennet et al. (2016) and can contribute to the ice melting identified in Schauwecker et al. (2014), Durán-Alarcón et al. (2015) and Berger et al. (2017). WSDI (Figure 9m) do not show a significant correlation with the elevation, but CSDI (Figure 9n) shows mostly a negative trend, which is related with the behaviour of the previous indices like TNn and TN10p (-0.26).

As mentioned, the latitudinal development of Northern Chile, ranges from 17º S to 29ºS, which allows a good visualization of the behaviour of different atmospheric variables in a wide latitudinal range over a relatively small territory. In this section, the relationship between temporal trends of indices and latitude was subjected to an analysis similar to the one conducted for elevation (Figure 10). According to Table 2, TXx and TNx (Figures 10a and 10b) show significant negative correlations with latitude (-0.55 and -0.32 respectively), which means that the more distance the stations are from the Equator, the more the decreasing trend rate is evident. The contrary happens with TNn, where less tropical stations show higher trend rates (Figure 10d). A similar pattern is observed according to percentile indices (Figures 10e, 10f, 10g and 10h). DTR shows a significant negative correlation with the latitude (Figure 10i), the same as SU25 (Figure 10k), with higher increases in the close-to-mid latitudes stations rather than inter-tropical ones (-0.61 and -0.56 respectively). The rise in warm episodes (WSDI) are more evident at high latitudes stations than at low latitudes (Figure 10m), which is evidenced by a significant negative correlation coefficient of -0.54. At higher latitudes, a general trend for warming is evidenced more by a decrease of persistent cold events, as shown in Figure 10n. These results disagree with those shown by Falvey and Garreaud (2009), since the global descent of warming rhythms may also be felt at the tropical coasts of South America, and agree partially with those presented by Karl et al. (2015), explained by linkage with the negative phase of the PDO. These findings could also be related to the sea surface temperatures of the Southeast Pacific (Kosaka and Xie 2013) but this outside the scope of this research.

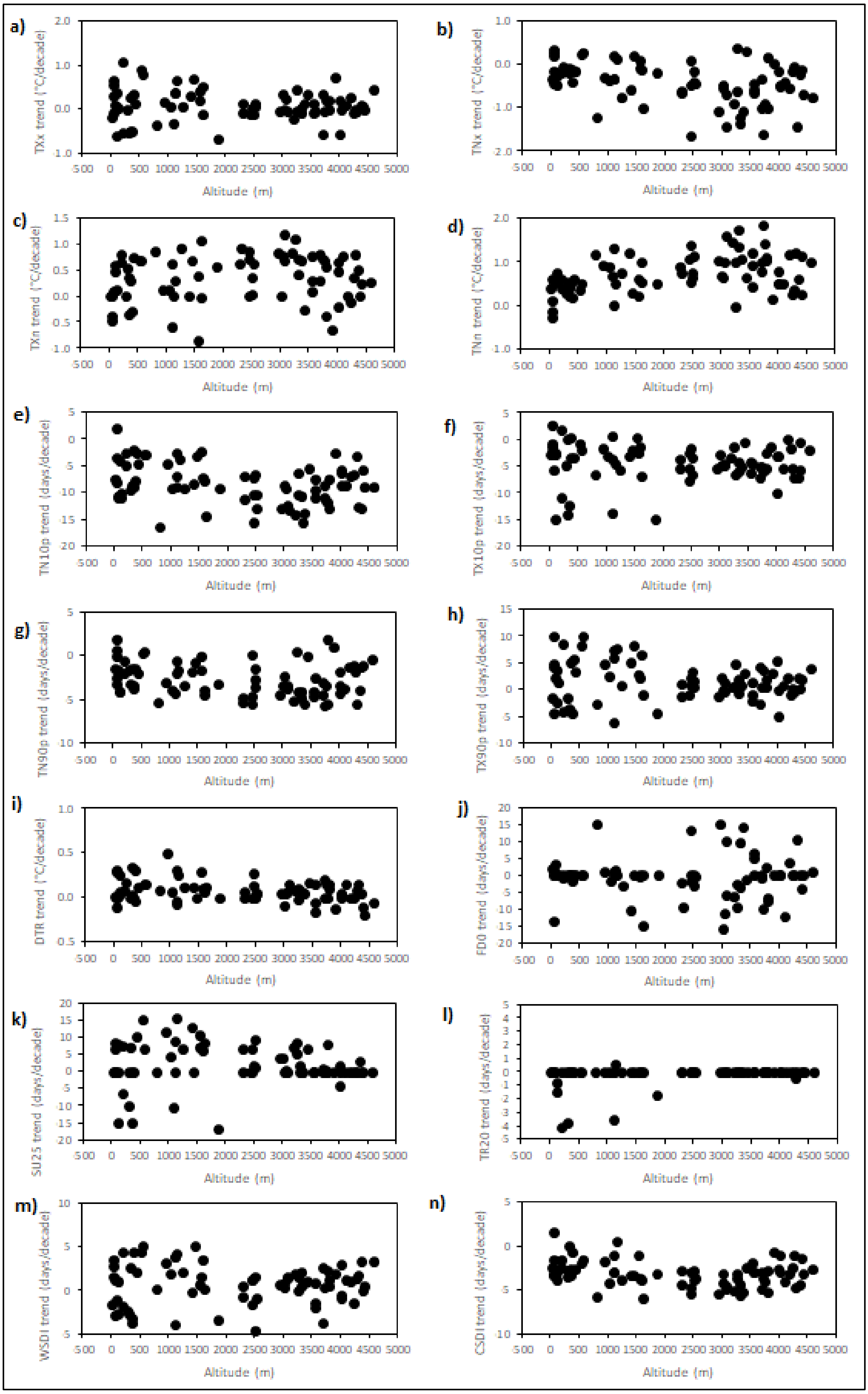

Fig. 9. The extreme temperature indices in relation to the elevation of stations

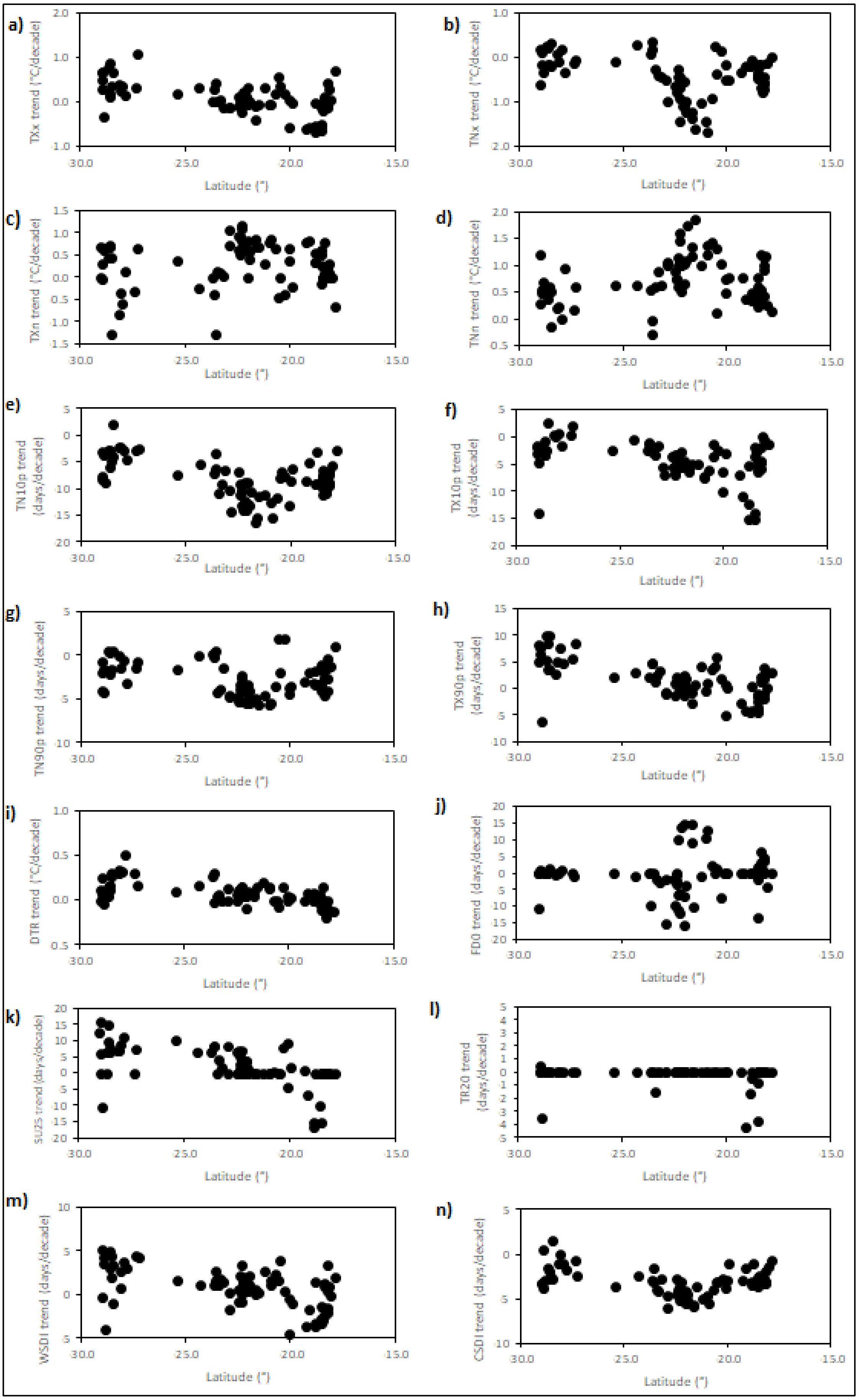

Fig. 10. The extreme temperature indices in relation to the latitude of stations

4. Conclusions

For a good study of temperature trends, a homogenization work is needed. In this case, for northern Chile, we were able to obtain 77 time series of daily maximum and minimum temperatures between 1966 and 2015.

General warming trends are evident in most of the planetary regions, and Northern Chile is not an exception to this, as it has been observed in several studies. This warming trends are linked in this case with the very evident rise of minimum temperatures. Maximum temperatures do not experiment a significative rise. But when using ETCDDI indices about extreme temperatures and focusing on regional scales, some particular behaviour of concrete stations may overcome. According to the maximum temperatures, the TXx and TXn indices show North-South differences, but both trends mark a warming behaviour, higher than 1ºC / decade depending on the observatory. However, in some observatories, the maximum values of minimum temperatures have decreased, mainly in the inter-tropical areas of Northern Chile, even reaching rates more intense than -1.5ºC / decade. According to percentile-based indices, the warming trends are not so evident in both minimum and maximum temperatures. The DTR index mainly shows significant positive trends (only one negative), which do not match with the general idea that global warming was mainly induced by rises in minimum temperatures, which is contrary to the results obtained here. The same happens with FD0, exhibiting more frequent frost days nowadays than in the mid-20th Century in several observatories in the north. Warm persistent events have decreased in the north also, but have increased in the centre and south of the study area. Cold persistent events show a very evident retreat over the whole territory. For each index, each meteorological station has a similar behaviour with each other, but for maximum temperature indices it tends to appear a latitudinal range between 20ºS and 22ºS where this behaviour is shifted. Altitude and latitude appear as two geographic variables strongly affecting extreme temperature indexes, while altitude more affects the minimum temperature based indices than maximum temperatures. On the other hand, latitude affects all indices in similar ways.

Generally, warming trends have been identified in the study area, but with some exceptions depending on the behaviour of the minimum temperature. However, the heterogeneity of temporal trends of indices and the multitude of factors affecting the high elevation means is yet to be determined. Therefore the exact mechanism influencing the variability of temporal trends of indices cannot be generalized across the entire area. The lack of a dense network of stations limits understanding how the elevation–warming trend relationships and therefore predicting the future patterns of these trends. Therefore, more stations are required to expand this study. Moreover, different responses of extreme temperatures have been identified depending on latitude and/or elevation, which evidences the effect of the region's complex orography in temperatures and therefor in climate. This needs to be considered to develop realistic and efficient policies concerning water management. This study will permit a more thorough analysis to better understand how general warming trends behalf on a region with a very complex orography and with regional and local particularities. Also will allow in future studies to determine how climate change impacts on the regional hydrological cycle so it will be possible to provide better tools to improve water management in arid areas of the region. Derived values from this investigation could be useful to more accurately quantify the temperature range for glacier-hydro-climatic and ecological modelling in the future.

Acknowledgements

The authors want to thank the FONDECYT Project 11160059, the UTA-Mayor Project 5755-17, the CLICES Project (CGL2017-83866-C3-2-R) and the Climatology Group (2014SGR300, Catalan Government). The authors would also thank Dr. Roberto Serrano-Notivoli (Barcelona Supercomputing Center) for his help.

Supporting information

The following supporting information is available for interested readers. Please, contact the corresponding author to request it::

TXxScript: R script to determine the extreme temperature values needed to calculate the TXx trends
TNxScript: R script to determine the extreme temperature values needed to calculate the TNx trends
TXnScript: R script to determine the extreme temperature values needed to calculate the TXn trends
TNnScript: R script to determine the extreme temperature values needed to calculate the TNn trends
TN10pScript: R script to determine the number of days at the 10th percentile of minimum temperatures needed to calculate the TN10p trends
TX10pScript: R script to determine the number of days at the 10th percentile of maximum temperatures needed to calculate the TX10p trends
TN90pScript: R script to determine the number of days at the 90th percentile of minimum temperatures needed to calculate the TN90p trends

TX90pScript: R script to determine the number of days at the 90^{th} percentile of maximum temperatures needed to calculate the TN90p trends

DTRScript: R script to calculate the monthly mean difference between daily maximum and minimum temperature to determine the DTR trends

FD0Script: R script to define the annual account of daily minimum temperature below 0º C to determine the FD0 trends

SU25Script: R script to define the annual account of daily maximum temperature above 25º C to determine the SU25 trends

TR20Script: R script to define the annual account of daily minimum temperature above 20º C to determine the TR20 trends

WSDIScript: R script to count annually the number of events of at least six consecutive days of maximum temperature > 90th percentile

CSDIScript: R script to count annually the number of events of at least six consecutive days of minimum temperature < 10th percentile

References

Abatan AA, Abiodun BJ, Gutowski Jr. WJ, Rasaq-Balogun SO (2017) Trends and variability in absolute indices of temperature extremes over Nigeria: linkage with NAO. Int J Climatol. doi: 10.1002/joc.5196

Alexandersson H (1986) A homogeneity test applied to precipitation data. Int J Climatol 6:661-675. doi: 10.1002/joc.3370060607

Alexandersson H, Moberg A (1997) Homogenization of Swedish temperature data. Part I: Homogeneity test for linear trends. Int. J. Climatol 17:25-34. doi: 10.1002/(SICI)1097-0088(199701)17:1<25::AID-JOC103>3.0.CO;2-J

Barkhordarian A, von Storch H, Zorita E, Loikith PC, Mechoso CR (2017) Observed warming over northern South America has an anthropogenic origin. Clim Dyn. doi: 10.1007/s00382-017-3988-z

Bennett M, New M, Marino J, Sillero-Zubiri C (2016) Climate complexity in the Central Andes: A study case on empirically-based local variations in the dry Puna. J Arid Environ 128:40-49. doi: 10.1016/j.jaridenv.2016.01.004

Beniston M, Diaz HF, Bradley RS (1997) Climatic Change at High Elevation Sites: An Overview. In: Diaz HF, Beniston M, Bradley RS (eds) Climatic Change at High Elevation Sites. Springer, Dordrecht. doi: doi.org/10.1007/978-94-015-8905-5_1

Berger A, Yin Q, Nifenecker H, Poitou J (2017) Slowdown of global surface air temperature increase and acceleration of ice melting. Earths Future. doi: 10.1002/2017EF000554

Berman AL, Silvestri G, Compagnucci R (2013) On the variability of seasonal temperature in southern South America. Clim Dyn 40:1863–1878. doi: 10.1007/s00382-012-1596-5

Burger F, Brock B, Montecinos A (2018) Seasonal and elevational contrasts in temperature trends in Central Chile between 1979 and 2015. Gobal Planet Change. doi: 10.1016/j.gloplacha.2018.01.005

Caloiero T (2016) Trend of monthly temperature and daily extreme temperature during 1951–2012 in New Zealand. Theor Appl Climatol. doi: 10.1007/s00704-016-1764-3

Caloiero T, Coscarelli R, Ferrari E, Sirangelo B (2017) Trend analysis of monthly mean values and extreme indices of daily temperature in a region of southern Italy. Int J Climatol. doi: 10.1002/joc.5003

Cai D, You Q, Fraedrich K, Guan Y (2017) Spatiotemporal Temperature Variability over the Tibetan Plateau: Altitudinal Dependence Associated with the Global Warming Hiatus. J Clim 30: 969-984. doi: 10.1175/JCLI-D-16-0343.1

Cowtan K, Way RG (2014) Coverage bias in the HadCRUT4 temperature series and its impact on recent temperature trends. Q J Roy Meteor Soc 140:1935-1944. doi: 10.1002/qj.2297

Durán-Alarcón C, Gevaert CM, Mattar C, Jiménez-Muñoz JC, Pasapera-Gonzales JJ, Sobrino JA, Silvia-Vidal Y, Fashé-Raymundo O, Chavez-Espiritu TW, Santillan-Portilla N (2015) Recent trends on glacier area retreat over the group of Nevados Caullaraju-Pastoruri (Cordillera Blanca, Peru) using Landsat imagery. J S Am Earth Sci 59:19-26. doi: 10.1016/j.jsames.2015.01.006

Donat M, Lowry A, Alexander L, O'Gorman P, Maher N (2016) More extreme precipitation in the world's dry and wet regions. Nat Clim Change 6:508-513. doi: 10.1038/NCLIMATE2941

England MH, McGregor S, Spence P, Meehl GA, Timmermann A, Cai W, Gupta AS, McPhaden MJ, Purich A, Santoso A (2014) Recent intensification of wind-driven circulation in the Pacific and the ongoing warming hiatus. Nat Clim Change 4:222-227. doi: 10.1038/nclimate2106

Falvey M, Garreaud RD (2009) Regional cooling in a warming world: Recent temperature trends in the southeast Pacific and along the west coast of subtropical South America (1979–2006). J Geophys Res 114:D04102. doi: 10.1029/2008JD010519

Feng R, Yu R, Zheng H, Gan M (2017) Spatial and temporal variations in extreme temperatures in Central Asia. Int J Climatol. doi: 10.1002/joc.5379

Frich P, Alexander LV, Della-Marta P, Gleason B, Haylock M, Klein Tank AMG, Peterson T (2002) Observed coherent changes in climatic extremes during the second half of the twentieth century. Clim Res 19: 193-212. doi: 10.3354/cr019193

Gabaldón-Leal C, Ruiz-Ramos M, de la Rosa R, León L, Belaj A, Rodríguez A, Santos C, Lorite IJ (2017) Impact of changes in mean and extremes temperatures caused by climate change on olive flowering in southern Spain. Int J Climatol. doi: 10.1002/joc.5048

Guan Y, Zhang X, Zheng F, Wang B (2015) Trends and variability of daily temperature extremes during 1960-2012 in the Yangtze River Basin, China. Global Planet Change 124:79-94. doi: 10.1016/j.gloplacha.2014.11.008

Guemas V, Doblas-Reyes FJ, Andreu-Burillo I, Asif M (2013) Retrospective prediction of the global warming slowdown in the past decade. Nat Clim Change 3: 649-653. doi: 10.1038/nclimate1863

Guijarro JA (2016) Package “climatol” Climate Tools (Series Homogenization and Derived Products). https://CRAN.R-project.org/package=climatol

Guijarro JA (2018) Homogenization of climate series with Climatol. Last accessed: May 2018. http://www.climatol.eu/homog_climatol-en.pdf

Held IM, Soden BJ (2006) Robust Responses of the Hydrological Cycle to Global Warming. J Climate 19:5686-5699. doi: 10.1175/JCLI3990.1

IPCC (2013) Summary for policymakers, Fifth Assessment Report of the Intergovernmental Panel on Climate Change. Cambridge University Press, Cambridge

Jacques-Coper M, Brönnimann S (2014) Summer temperature in the eastern part of southern South America: its variability in the twentieth century and a teleconnection with Oceania. Clim Dyn 43:2111–2130. doi: 10.1007/s00382-013-2038-8

Karl TR, Arguez A, Huang B, Lawrimore JH, McMahon JR, Menne MJ, Peterson TC, Vose RS, Zhang HM (2015) Possible artifacts of data biases in the recent global surface warming hiatus. Science 348 (6242):1469-1472. doi: 10.1126/science.aaa5632

Kattel DB, Yao T (2018) Temperature–topographic elevation relationship for high mountain terrain: an example from the southeastern Tibetan Plateau. Int j Climatol. doi: 10.1002/joc.5418

Keellings D, Waylen P (2012) The stochastic properties of high daily maximum temperatures applying crossing theory to modelling high-temperature event variables. Theor Appl Climatol 108:579-590. doi: 10.1007/s00704-011-0553-2

Kendall MG (1962) Rank correlation methods. Hafner Publishing Company, New York

Khaliq MN, Ouarda TBMJ (2007) On the critical values of the standard normal homogeneity test (SNHT). Int. J. Climatol., 27:681-687. doi: 10.1002/joc.1438

Klein Tank AMG, Wijngaard JB, Koennen GP, Boehm R, Demaree G, Gocheva A, Mileta M, Pashiardis S, Hejkrlik L, Kern-Hansen C (2002) Daily surface air temperature and precipitation dataset 1901–1999 for European Climate Assessment (ECA). Int J Climatol 22(12): 1441-1453. doi: 10.1002/joc.773

Kosaka Y, Xie SP (2013) Recent global-warming hiatus tied to equatorial Pacific surface-cooling. Nature 501:403-407. doi: 10.1038/nature12534

Labat D, Goddéris Y, Probst JL, Guyot JL (2004) Evidence for global runoff increase related to climate warming. Adv Water Resour 27:631-642. doi: 10.1016/j.advwatres.2004.02.020

Lavado Casimiro WS, Labat D, Ronchail J, Espinoza JC, Guyot JL (2013) Trends in rainfall and temperature in the Peruvian Amazon-Andes basin over the last 40 years (1965–2007). Hydrol Process 41:2944-2957. doi: 10.1002/hyp.9418

Liang K, Bai P, Li J, Liu C (2014) Variability of temperature extremes in the Yellow River basin during 1961-2011. Quatern Int 336: 52-64. doi: 10.1016/j.quaint.2014.02.007

Mann HB (1945) Nonparametric tests against trend. Econometrica 13: 245-259. doi: 0012-9682(194507)13:3<245:NTAT>2.0.CO;2-U

Maraun D, Huth R, Gutiérrez JM, San Martín D, Dubrovsky M, Fischer A, Hertig E, Soares PMM, Bartholy J, Pongrácz R, Widmann M, Casado MJ, Ramos P, Bedia J (2017) The VALUE perfect predictor experiment: evaluation of temporal variability. Int J Climatol. doi: 10.1002/joc.5222

Marengo JA, Pabón JD, Díaz A, Rosas G, Ávalos G, Montealegre E, Villacis M, Solman S, Rojas M (2011) Climate change: Evidence and future scenarios for the Andean region. In: Herzog SK, Martínez R, Jørgensen PM, Tiessen H (eds) Climate Change and Biodiversity in the Tropical Andes. Inter-American Institute for Global Change Research SCOPE Publication, Sao Paulo, pp 110-127

Meehl GA, Arblaster JA, Fasullo JT, Hu A, Trenberth KE (2011) Model-based evidence of deep-ocean heat uptake during surface temperature hiatus periods. Nat Clim Change 1:360-364. doi: 10.1038/nclimate1229

Meehl GA, Teng H, Arblaster JA (2014) Climate model simulations of the observed early-2000s hiatus of global warming. Nat Clim Change 4:898-902. doi: 10.1038/nclimate2357

Otto A, Otto FEL, Boucher O, Church J, Hegerl G, Forster PM, Gillet NP, Gregory J, Johnson GC, Knutti R, Lewis N, Lohman U, Marotzke J, Myhre G, Shindell D, Stevens B, Allen MR (2013) Energy budget constraints on climate response. Nat Geosci 6:415-416. doi: 10.1038/ngeo1836

Parak F, Roshani A, Rehmani MIA (2015) Trends and Anomalies in Daily Climate Extremes over Iran during 1961–2010. Journal of Environmental and Agricultural Sciences 2:11. doi:

Poveda G, Pineda K (2009) Reassessment of Colombia’s tropical glaciers retreat rates: Are they bound to disappear during the 2010–2020 decade? Advances in Geosciences 22:107-116. doi: 10.5194/adgeo-22-107-2009

Rabatel A, Francou B, Soruco A, Gomez J, Caceres B, Ceballos JL, Basantes R, Vuille M, Sicart JE, Huggel C, Scheel M, Lejeune Y, Arnaud Y, Collet M, Condom T, Consoli G, Favier V, Jomelli V, Galarraga R, Ginot P, Maisincho L, Mendoza J, Menegoz M, Ramirez E, Ribstein P, Suarez W, Villacis M, Wagnon, P (2013) Current state of glaciers in the tropical Andes: A multi-century perspective on glacier evolution and climate change. Cryosphere 7:81-102. doi:10.5194/tc-7-81-2013

Rahimi M, Hejabi S (2017) Spatial and temporal analysis of trends in extreme temperature indices in Iran over the period 1960-2014. Int J Climatol. doi: 10.1002/joc.5175

Rosenblüth B, Fuenzalida HA, Aceituno P (1997) Recent temperature variations in southern South America. Int J Climatol 17:67-85. doi: 10.1002/(SICI)1097-0088(199701)17:1<67::AID-JOC120>3.0.CO;2-G

Salman SA, Shahid S, Ismail T, Chung ES, Al-Abadi AM (2017) Long-term trends in daily temperature extremes in Iraq. Atmos Res 198:97-107. doi: 10.1016/j.atmosres.2017.08.011

Salmi T, Määttä A, Anttila P, Ruoho-Airola T, Amnell T (2002) Detecting trends of annual values of atmospheric pollutants by the Mann–Kendall test and Sen’s slope estimates the Excel template application MAKESENS. Ilmatieteen laitos, Meteorologiska Institutet, Finnish Meteorological Institute

Salzmann N, Huggel C, Rohrer M, Silverio W, Mark BG, Burns P, Portocarrero C (2013) Glacier changes and climate trends derived from multiple sources in the data scarce Cordillera Vilcanota region, southern Peruvian Andes. Cryosphere 7:103-118. doi: 10.5194/tc-7-103-2013

Santer BD, Bonfils C, Painter JF, Zelinka MD, Mears C, Solomon S, Schmidt GA, Fyfe JC, Cole JNS, Nazarenko L, Taylor KE, Wentz FJ (2014) Volcanic contribution to decadal changes in tropospheric temperature. Nat Geosci 7:185-189. doi: 10.1038/ngeo2098

Sarricolea P, Romero Aravena H (2015) Variabilidad y cambios climáticos observados y esperados en el Altiplano del norte de Chile. Rev Geogr Norte Gd 62:169-183

Sarricolea P, Herrera-Ossandon MJ, Meseguer-Ruiz O (2017) Climatic Regionalisation of Continental Chile. J Maps 13(2):66-73. doi: 10.1080/17445647.2016.1259592

Schauwecker S, Rohrer M, Acuña D, Cochachin A, Dávila L, Frey H, Giráldez C, Gómez J, Huggel C, Jacques-Coper M, Loarte E, Salzmann N, Vuille M (2014) Climate trends and glacier retreat in the Cordillera Blanca, Peru, revisited. Global Planet Change 119:85-97. doi: 10.1016/j.gloplacha.2014.05.005

Schauwecker S, Rohrer M, Huggel C, Endries J, Montoya N, Neukom R, Perry B, Salzmann N, Schwarb M, Suarez W (2017) The freezing level in the tropical Andes, Peru: An indicator for present and future glacier extents. J Geophys Res-Atmos 122:5172-5189. doi: 10.1002/2016JD025943

Schulz N, Bosier, JP, Aceituno P (2012) Climate change along the arid coast of northern Chile. Int J Climatol 32(12):1803-1814. doi: 10.1002/joc.2395

Seiler C, Hutjes RWA, Kabat P (2013) Climate variability and trends in Bolivia. J Appl Meteorol Clim, 52:1303-1317. doi: 10.1175/JAMC-D-12-0105.1

Sen PK (1968) Estimates of the regression coefficient based on Kendall’s tau. J Am Stat Assoc, 63:1379-1389. doi: 10.2307/2285891

Shen X, Liu B, Lu X, Fan G (2017) Spatial and temporal changes in daily temperature extremes in China during 1960–2011. Theor Appl Climatol 130: 933-943. doi: 10.1007/s00704-016-1934-3

Shresta AB, Bajracharya SR, Sharma AR, Duo C, Kulkarni A (2017) Observed trends and changes in daily temperature and precipitation extremes over the Koshi river basin 1975–2010. Int J Climatol 37: 1066-1083. doi: 10.1002/joc.4761

Solomon S, Daniel JS, Neely RR, Vernier JP, Dutton EG, Thomason LW (2011) The persistently variable “background” stratospheric aerosol layer and global climate change. Science 333(6044):866-870. doi: 10.1126/science.1206027

Szentimrey, T (2013) Theoretical questions of daily data homogenization. Idöjárás, 117:113-122.

Tao H, Fraedrich K, Menz C, Zhai J (2014) Trends in extreme temperature indices in the Poyang Lake Basin, China. Stoch Environ Res Risk Assess 28: 1543-1553. doi: 10.1007/s00477-014-0863-x

Thibeault JM, Seth A, Garcia M (2010) Changing climate in the Bolivian Altiplano: CMIP3 projections for temperature and precipitation extremes. J Geophys Res 115: D08103. doi: 10.1029/2009JD012718

Tian J, Liu J, Wang J, Li C, Nie H, Yu F (2017) Trend analysis of temperature and precipitation extremes in major grain producing area of China. Int J Climatol. doi: 10.1002/joc.4732

Trenberth KE, Jones PD, Ambenje P, Bojariu R, Easterling D, Klein Tank A, Parker D, Rahimzadeh F, Renwick JA, Rusticucci M, Soden B, Zhai P (2007) Observations: surface and atmospheric climate change. In: Climate Change 2007: The Physical Science Basis. Contribution of Working Group I to the Fourth Assessment Report of the Intergovernmental Panel on Climate Change, Solomon S, Qin D, Manning M, Chen Z, Marquis M, Averyt KB, Tignor M, Miller HL (eds). Cambridge University Press: Cambridge, UK and New York, NY.

Trenberth KE, Fasullo JT (2013) An apparent hiatus in global warming? Earths Future 1:19-32. doi: 10.1002/2013EF000165

Vicente-Serrano SM, López-Moreno JI, Correa K, Avalos G, bazo J, Azorin-Molina C, Domínguez-Castro F, El Kenawy A, Gimeno L, Nieto R (2017) Recent changes in monthly surface air temperature over Peru, 1964-2014. Int J Climatol. doi: 10.1002/joc.5176

Villarini G, Khouakhi A, Cunningham E (2017) On the impacts of computing daily temperatures as the average of the daily minimum and maximum temperatures. Atmos Res 198:145-150. doi: 10.1016/j.atmosres.2017.08.020

Vose RS, Easterling DR, Gleason B (2005) Maximum and minimum temperature trends for the globe: an update through 2004. Geophys Res Lett 32:L23822. doi: 10.1029/2005GL024379

Vuille M, Bradley RS (2000) Mean annual temperature trends and their vertical structure in the tropical Andes. Geophys Res Lett 27:3885-3888. doi: 10.1029/2000GL011871

Vuille M, Franquist E, Garreaud R, Lavado Casimiro WS, Cáceres B (2015) Impact of the global warming hiatus on Andean temperature. J Geophy Res-Atmos 120:3745-3757. doi: 10.1002/2015JD023126

Ye L, Yang G, Van Ranst E, Tang H (2013) Time-series modelling and prediction of global monthly absolute temperature for environmental decision making. Adv Atmos Sci 30:382-396. doi: 10.1007/s00376-012-1252-3

Zhai PM, Zhang XB, Wan H, Pan XH (2005) Trends in total precipitation and frequency of daily precipitation extremes over China. J Climate 18:1096-1108. doi: 10.1175/JCLI-3318.1

Zhang X, Alexander L, Hegerl GC, Jones P, Tank AK, Peterson TC, Trewin B, Zwiers FW (2011) Indices for monitoring changes in extremes based on daily temperature and precipitation data. WIREs Clim Change 2:851-870. doi: 10.1002/wcc.147